



24th COBEM - 2017



24th ABCM International Congress of Mechanical Engineering
December 3-8, 2017, Curitiba, PR, Brazil

COBEM-2017-2395

FATIGUE LIMIT DETERMINATION OF A LOW CARBON STEEL USING THE THERMOGRAPHIC TECHNIQUE

Carlos Filipe Cardoso Bandeira

Centro Federal de Educação Tecnológica Celso Suckow da Fonseca – Programa de Pós Graduação em Engenharia Mecânica e Tecnologia de Materiais – Rio de Janeiro/RJ, Brasil
filypebandeira@hotmail.com

Paulo Pedro Kenedi

Centro Federal de Educação Tecnológica Celso Suckow da Fonseca – Programa de Pós Graduação em Engenharia Mecânica e Tecnologia de Materiais – Rio de Janeiro/RJ, Brasil
ppkenedi@gmail.com

Jaime Tupiassú Pinho de Castro

Pontifícia Universidade Católica do Rio de Janeiro – Departamento de Engenharia Mecânica – Rio de Janeiro/RJ, Brasil
jtcastro@puc-rio.br

Abstract. *Traditional methods to obtain the fatigue limit of materials are expensive and time consuming, requiring a considerable number of specimens and a long time to be completed. In this work, the thermographic technique is applied to determine the fatigue limit of a low carbon steel, using an infrared camera. The traditional staircase method is also used as reference to check thermography performance. The results show that thermography technique is really faster than staircase to determine the fatigue limit of this material.*

Keywords: *fatigue limit, thermography, staircase*

1. INTRODUCTION

Traditional experimental methods to determine the fatigue limit of materials (S_L) are laborious, expensive, time consuming and require a large number of specimen to be completed as, for instance, the staircase which depends on the total number of tested specimens (n_T) and on the number of cycles for infinite life characterization (N_∞).

The staircase starts loading the first specimen under a stress amplitude (σ_{a0}) close to the expected fatigue limit for material (S_{L-exp}). If it survives after a determined number of cycles (N_∞), the next one is tested under a higher stress amplitude (σ_{a1}) increased by a constant stress amplitude increment ($s = \Delta\sigma_a$), as shown in Eq. (1). However if the specimen breaks before achieve the infinity life criteria, the next one is tested under a lower stress amplitude decreased by the same value as in Eq. (2), Nicholas (2006). This iteration continues until all specimens are tested.

$$\sigma_{a1} = \sigma_{a0} + s \quad (1)$$

$$\sigma_{a1} = \sigma_{a0} - s \quad (2)$$

After all specimens have been tested, the statistical calculation proposed by Dixon and Mood is used to determine the mean (\bar{X}) and the standard deviation (ϕ) of the fatigue limit. It depends on the less frequent event (*LFE*) during the tests, specimen's failure or survival, with more conservative equations if *LFE* = survival and less conservative equations if *LFE* = failure, Pollak, *et al.* (2006).

There are many important points that need to be highlighted about staircase, despite being a relatively widespread method for experimental fatigue limit determination. For example: the guess for the first stress amplitude (σ_{a0}) is important to accelerate the convergence value of S_L ; the loading frequency (f) is fundamental because a single specimen can take days to be tested depending on its value; the choice of the number of cycles for infinite life characterization is critical (i.e. $N_\infty = 1 \cdot 10^6$ cycles for carbon steels could be not representative); the stress amplitude increment (s) and the total tested specimens (n_T) also influence the test performance.

The thermographic technique is proposed to be a faster experimental way to determine the fatigue limit of materials, mitigating the drawbacks previously exposed. This technique uses the correlation between the cyclic loading and the energy released into material, described by a temperature variation (ΔT) or by a temperature increase rate ($\partial T/\partial N$) on specimen's surface. These variations are measured under several stress amplitudes (n_t), from lower to higher values in relation to the expected fatigue limit (loading history), each one of them for the number of cycles necessary to achieve the second thermal phase (N_f) on a same specimen (see Fig. 6a), in order to correlate $\Delta T \times \sigma_a$ or $\partial T/\partial N \times \sigma_a$. With either of these correlations the fatigue limit can be determined making $\Delta T = 0$ or $\partial T/\partial N = 0$, la Rosa, *et al.* (2000).

From a statistical point of view, is it reasonable testing at least three specimens under the same loading history in order to determine the mean and standard deviation of the fatigue limit. Figure 1 shows a flowchart with the thermographic technique, where i and k are integer counters ($i \geq 0$ and $k \geq 0$).

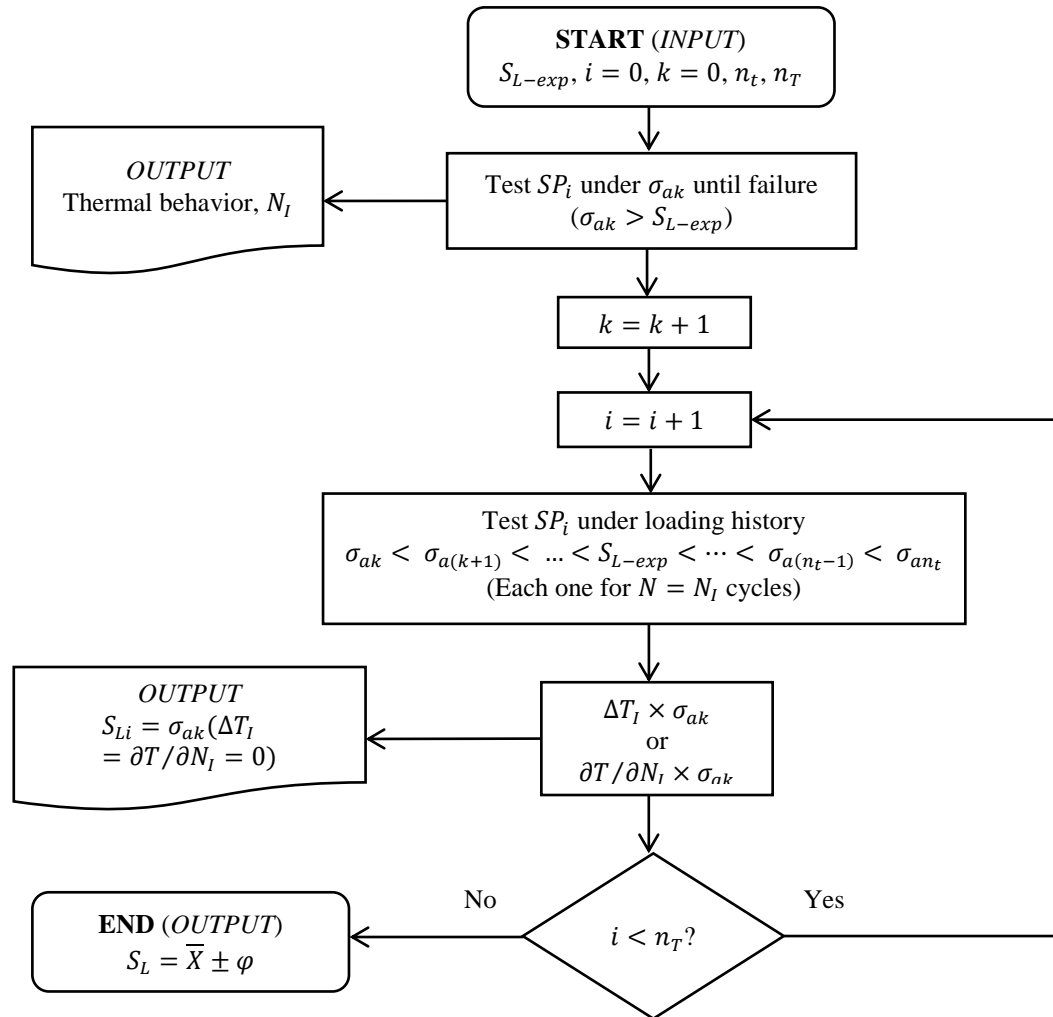


Figure 1. Fatigue limit determination by thermographic technique

Important points can also be highlighted regarding to the thermographic technique. For example: the loading frequency (f), because depending on the material and the stress amplitude it has to be high enough to generate measurable temperatures; if infrared camera is used to measure temperature fields, some actions have to be done in order to improve camera performance, like painting specimen with a black ink to increase its emissivity; if a thermocouple is used to measure temperature, is very important to check during the tests if some crack started and is propagating into material, because in this case the temperature read by thermocouple is not representative.

In this work, the thermographic technique is used to determine the fatigue limit of a low carbon steel, correlating the temperature increase rate with stress amplitude ($\partial T/\partial N \times \sigma_a$). For this, round specimens are tested under rotating bending and temperature measurements are taken by an infrared camera FLIR A320. In order to check thermography performance, traditional staircase method is also performed.

2. MATERIAL AND METHODS

To perform thermography and staircase approaches, specimens of low carbon steel were taken from cold drawn round bars of the same manufacturing batch. The tensile mechanical properties of this material are presented in the Tab. 1. The specimens were designed according to standard ASTM E466, with hourglass geometry, and were machined using a CNC lathe in order to increase dimensions repeatability. The specimen's middle region has an average roughness of $R_a = 0.78 \mu\text{m}$, achieved through a fine control of the last machining pass. Figure 2a shows the specimen geometry and dimensions.

Table 1. Tensile mechanical properties

| Yield Strength, S_y (MPa) | Tensile Strength, S_{ut} (MPa) | Elongation (%) | Area Reduction (%) |
|-----------------------------|----------------------------------|----------------|--------------------|
| 576.6 | 666.6 | 14.5 | 50.1 |

All fatigue tests were performed in a rotating bending machine RBF 200, shown in Fig. 2b, with a loading ratio of $R = -1$ and angular frequency of $f = 8500 \text{ rpm}$. For thermography technique the temperature variation was measured by an infrared camera FLIR A320 with a resolution of 320×240 pixels and a temperature sensitivity of 30 mK .

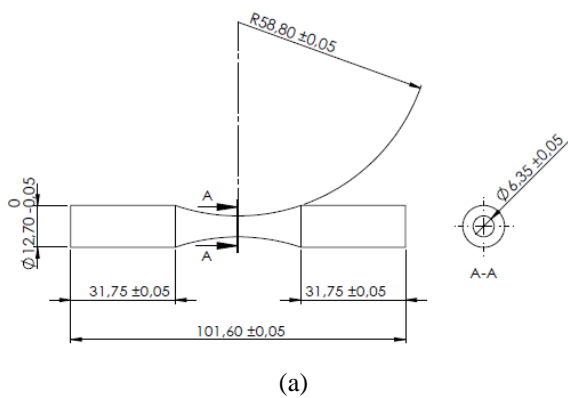


Figure 2. Fatigue test: (a) specimen geometry (dimension in mm); (b) rotating bending machine RBF 200

Some precautions were adopted in order to improve camera performance, like covering acquisition system with a black cloth and painting specimen's central region with a black ink, as shown in Fig. 3.

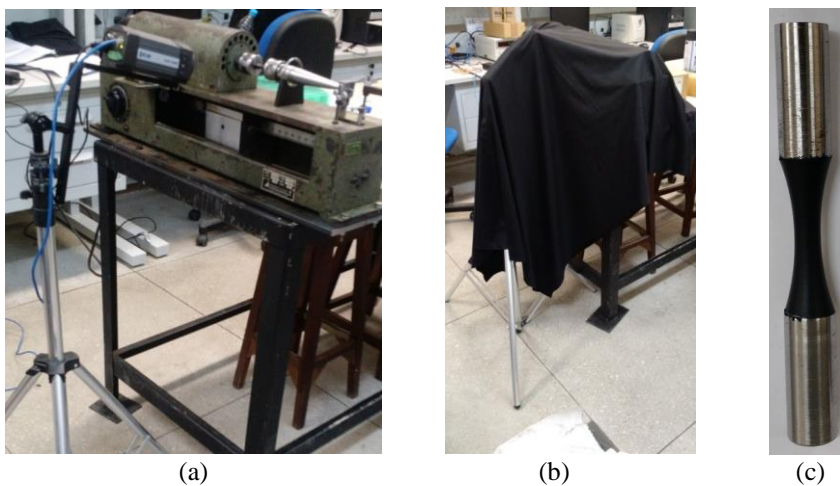


Figure 3. Thermography system: (a) infrared camera + RBF 200; (b) black cloth; (c) painted specimen

All stress amplitude used on fatigue tests are represented as a ratio with material tensile strength (S_{ut}), as in Eq. (3).

$$\sigma_a = (\sigma_a / S_{ut}) \cdot 100\% \quad (3)$$

The staircase method is started with a stress amplitude of $\sigma_{a0}/S_{ut} = 40\%$, a guess due to the high material tensile strength and the good surface finish of specimen's critical region. The stress amplitude increment is set to $s = 2\%$, a low value to increase the accuracy of result. It is considered as surviving specimens those that reach $N_{\infty} = 5 \times 10^6$ cycles. This value is arbitrarily chosen (provided that was greater than 1×10^6 cycles) according to the maximum number of cycles that is possible to achieve in the laboratory for a workday of 10 hours, under the test loading frequency. For staircase approach 25 specimens are tested ($n_T = 25$) in about 22 days. The mean (\bar{X}) and the standard deviation (φ) of the fatigue limit determined by it (S_{LS}) are calculated by Dixon and Mood statistical purpose.

The thermography approach is implemented in three stages. The first one is to characterize the material temperature variation until failure, under different stress amplitudes, in order to define its thermal behaviour under cyclic loading. At this same stage, it is defined the number of cycles to reach the end of first thermal phase N_I , which will be used in the next stage. In the second, several stress amplitudes are performed on a same specimen, each one for N_I cycles, using an incremental loading sequence starting from $\sigma_{a0}/S_{ut} = 35\%$. For each stress amplitude is defined the temperature increase rate of the first thermal phase ($\partial T/\partial N_I$). The third and last stage is plotting the correlation $\partial T/\partial N_I \times \sigma_a/S_{ut}$ to fit a straight line through the highest temperature increase rates, determining the fatigue limit making $\partial T/\partial N_I = 0$.

The straight line fitting is here proposed to be done using as reference the first and lowest measurement of $\partial T/\partial N_I$ for $\sigma_{a0}/S_{ut} = 35\%$. The idea is to take into account only temperature increase rates higher than reference value by at least 10%, as in Eq. (4), where k is an integer counter ($k \geq 1$).

$$\left[\frac{\partial T/\partial N_I (\sigma_{ak}/S_{ut})}{\partial T/\partial N_I (\sigma_{a0}/S_{ut})} - 1 \right] \times 100\% \geq 10\% \quad (4)$$

In total, 5 specimens were tested with thermography approach ($n_T = 5$) under the same incremental loading path with 9 different stress amplitude levels ($n_t = 9$). The mean (\bar{X}) and the standard deviation (φ) of the fatigue limit determined by it (S_{LT}) are calculated by a simple statistical analysis, considering the results obtained for each specimen, as in Eq. (5) and (6) respectively.

$$\bar{X}_{S_{LT}} = \sum_{i=1}^{n_T} \left(\frac{S_{Li}}{n_T} \right) \quad (5)$$

$$\varphi_{S_{LT}} = \sqrt{\frac{\sum_{i=1}^{n_T} |S_{Li} - \bar{X}_{S_{LT}}|^2}{n_T}} \quad (6)$$

The next section shows the results obtained by each technique.

3. RESULTS

The fatigue limit results obtained with staircase and thermography approaches are presented in sequence.

3.1 Staircase

Figure 4 shows the results obtained with all 25 specimens, in the real test ordering. It is possible to note that stress amplitude varied from $40\% \leq \sigma_a/S_{ut} \leq 46\%$, although only the first specimen has been tested at the lowest loading and all at the highest level had failed. Anyway the results are in a short range of three times the amplitude stress increment previously determined ($3 \times s$). In addition, there were more survival specimens than failed ones (14 against 11) as a good indication that fatigue limit is into this range or very close to it boundaries.

Table 5, at Appendix, shows details of each specimen result. All failed specimens did not reach $N = 4 \times 10^6$ cycles, a lower value than the infinity life criteria previously defined ($N_{\infty} = 5 \times 10^6$ cycles). In addition, many of them supported at least $N = 1 \times 10^6$ cycles to failure, which means that if $N_{\infty} = 1 \times 10^6$ cycles was chosen, these specimens would have been characterized as survival instead of failed, which could affect the final fatigue limit result.

The results obtained were implemented into Dixon and Mood statistical purpose to determine the mean and standard deviation values of the fatigue limit. Table 2 presents the fatigue limit result according to the staircase approach (S_{LS}) both in terms of stress amplitude and of its ratio with tensile ultimate strength.

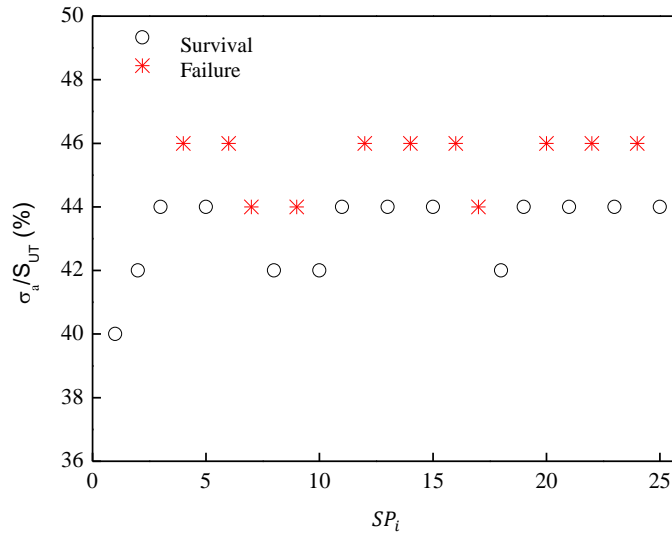


Figure 4. Staircase results

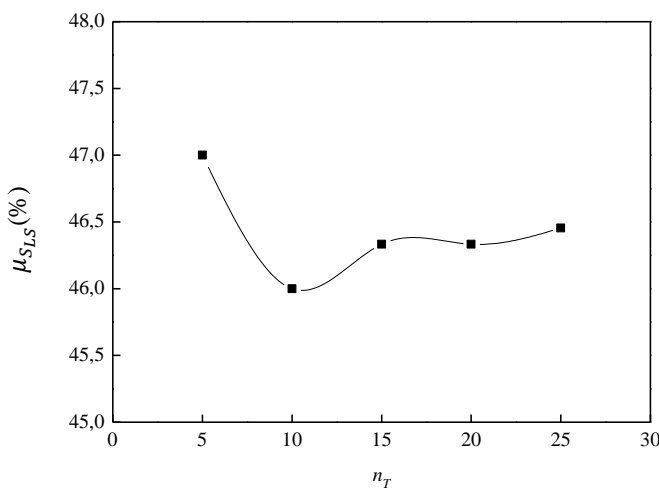
Table 2. Fatigue limit by staircase approach

| $\overline{X}_{S_{LS}}$ (%) | $\varphi_{S_{LS}}$ (%) | S_{LS} (MPa) |
|-----------------------------|------------------------|-----------------|
| 46,3 | 1,1 | $308,9 \pm 7,1$ |

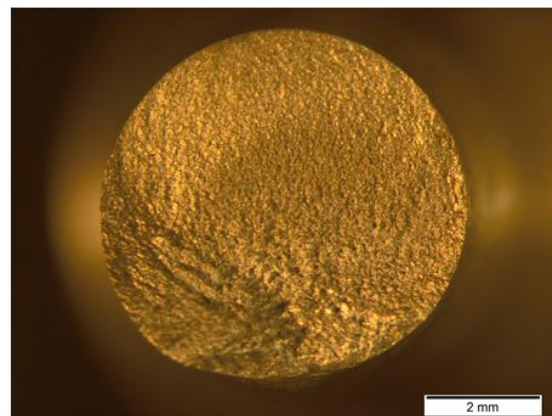
Table 2 shows that fatigue limit obtained through staircase technique is high and close to the expected value for a standard and polished specimen ($S_{L-est} = S_{ut}/2 = 333\text{MPa}$). In addition, the standard deviation is small and lower than the stress amplitude increment used during tests ($s = 2\%$), which represents a good accuracy of the method, after 22 days of testing.

In order to check the staircase sensitivity regarding to the total number of tested specimens (n_T) in the fatigue limit determination, it is considered $n_T = 5, 10, 15, 20$ and 25 specimens in the Dixon and Mood statistical calculation purpose. Figure 5a shows the $\overline{X}_{S_{LS}}$ as a function of n_T and shows that there is a convergence of the fatigue limit as the total number of tested specimens is increasing. The variation of the fatigue limit is small between $10 \leq n_T \leq 25$ specimens, which can be explained by the good guess for the first stress amplitude ($\sigma_{a0}/S_{ut} = 40\%$), by the small s -increment and also by the refined control of material and machining process.

To check the fracture surface under cyclic rotating bending, the specimen SP_7 is analyzed through a macrograph by magnifying glass, as shown in Fig. 5b. It failed after a large number of cycles (see Tab. 5) and under a stress amplitude of $\sigma_a/S_{ut} = 44\%$. It is possible to note that failure surface has a crack propagation area (flat region) larger than final fracture (rough region), commonly obtained on this kind of loading and stress amplitude level, de Castro *et al.* (2016).



(a)



(b)

Figure 5. (a) Staircase sensitivity in function of n_T and (b) Fracture surface macrograph of SP_7

3.2 Thermography

Figure 6a shows the material thermal behavior $T_{max} \times N$ obtained under $\sigma_{a0}/S_{ut} = 60\%$. Note that phase I is characterized by a small number of cycles ($N_I < 5 \times 10^3$ cycles); phase II is responsible for the most life of the specimen ($N_{II} \approx 2 \times 10^4$ cycles) and phase III is associated to a sudden temperature increase at which the specimen final fracture occurs in a small number of cycles ($N_{III} < N_I$).

Figure 6b shows some pictures of the temperature distribution on specimen's surface during three thermal phases until final rupture, under $\sigma_{a0}/S_{ut} = 60\%$. They show that, as expected, the highest temperature field is located around the smaller cross section of the specimen, with a gradient along longitudinal direction by thermal conduction during the tests.

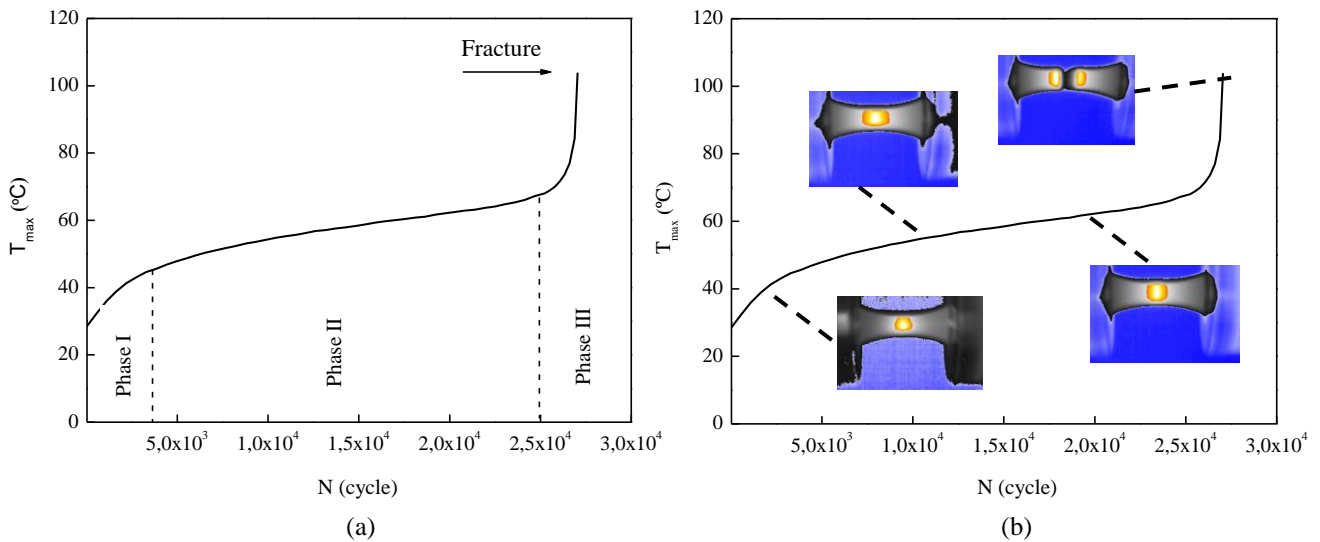


Figure 6. For $\sigma_{a0}/S_{ut} = 60\%$: (a) $T_{max} \times N$ behavior and (b) Temperature distribution

Figure 7a shows the incremental loading path performed on the second tested specimen SP_2 . Note that for low stress amplitude ratio the temperature increase rate is almost equal to zero, which represents no fatigue damage. For loading around $\sigma_a/S_{ut} = 44\%$ the temperature starts to increase, representing a possible fatigue damage phenomenon due to the heat release and consequently external temperature increasing.

The relation $\partial T/\partial N_I \times \sigma_a/S_{ut}$ for the second tested specimen SP_2 is presented by Fig. 7b. Note there is an almost bilinear trend with huge different slopes which characterize the transition *no fatigue damage* (where $\partial T/\partial N_I \approx 0$) to *fatigue damage* (where $\partial T/\partial N_I > 0$). It also shows the straight line fitted through experimental results which respect the condition established by Eq. (4) in order to determine the fatigue limit by thermography technique (S_{LT}).

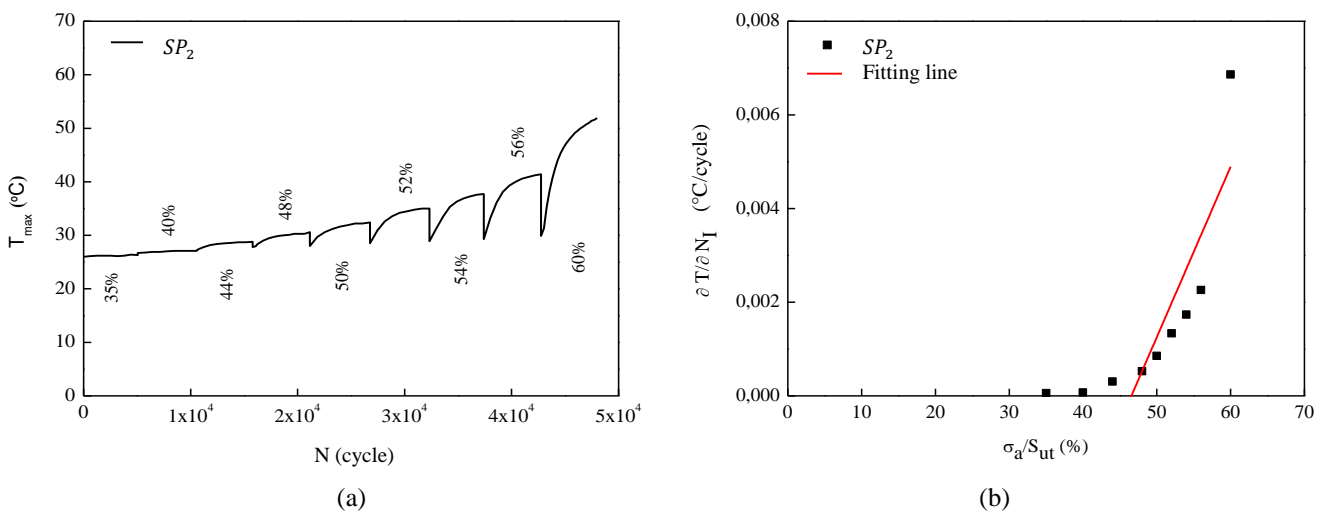


Figure 7. Second specimen SP_2 : (a) Loading path and (b) $\partial T/\partial N_I \times \sigma_a/S_{ut}$

The fatigue limit using thermography is determined for five specimens and the results are processed according to Eq. (5) and (6) to determine the mean value and standard deviation. Table 3 shows the results obtained. Note that thermography results presents a small standard deviation and a mean value very close to that obtained by staircase approach, which is a good performance result.

Table 3. Fatigue limit by thermography approach

| $\overline{X}_{S_{LT}}$ (%) | $\varphi_{S_{LT}}$ (%) | S_{LT} (MPa) |
|-----------------------------|------------------------|-----------------|
| 45.9 | 0.8 | 305.8 ± 5.3 |

The next section presents the conclusion obtained with results presented above.

4. CONCLUSION

The Table 4 summarizes the results obtained with both techniques used in this work: staircase and thermography.

Table 4. Summary of results

| Technique | Number of specimens | Total time (day) | Fatigue limit (MPa) |
|--------------|---------------------|------------------|---------------------|
| Staircase | 25 | 22 | 308.9 |
| Thermography | 5 | 3 | 305.8 |

Table 5 shows that thermography approach is a really faster method than staircase, since it required 1/5 fewer specimens and was performed in only 3 days compared to 22 days needed for staircase test 25 specimens. In addition, the fatigue limit obtained by thermography is very close to the staircase, with a nominal percentage difference less than 5%.

5. REFERENCES

- de Castro, J.T.P. and Meggiolaro, M.A., 2016. *Fatigue - Design Techniques under Real Service Loads*. Amazon Books, Charleston, Vol. I - High-Cycle Fatigue.
- Hou, P.; Fan, J.; Guo, Q.; Guo, X., 2014. "The application of the infrared thermography on titanium alloy for studying fatigue behavior", *Frattura ed Integrità Strutturale*, vol. 27, pp. 21-27.
- la Rosa, G.; Risitano, A., 2000. "Thermographic methodology for rapid determination of the fatigue limit of materials and mechanical components". *International Journal of Fatigue*, vol. 22, pp. 65-73.
- Nicholas, T., 2006. High cycle fatigue – A mechanics of materials perspective. Chapter 3, Elsevier, Great Britain.
- Pollak, R.; Palazotto, A.; Nicholas, T., 2006, "A simulation-based investigation of the staircase method for fatigue strength testing", *Mechanics of Material*, 38, pp.1170-1181.

6. RESPONSIBILITY NOTICE

The authors are the only responsible for the printed material included in this paper.

7. APPENDIX

Table 5. Staircase detailed results

| SP_i | σ_a/S_{ut} (%) | N (cycles) | Final situation |
|--------|-----------------------|-------------------|-----------------|
| 1 | 40 | 6×10^6 | Survival |
| 2 | 42 | 5.5×10^6 | Survival |
| 3 | 44 | 5.3×10^6 | Survival |
| 4 | 46 | 2×10^6 | Failure |
| 5 | 44 | 1×10^7 | Survival |
| 6 | 46 | 8.1×10^5 | Failure |
| 7 | 44 | 3.8×10^6 | Failure |
| 8 | 42 | 5×10^6 | Survival |
| 9 | 44 | 2.7×10^6 | Failure |
| 10 | 42 | 5.7×10^6 | Survival |
| 11 | 44 | 5.9×10^6 | Survival |
| 12 | 46 | 9.7×10^5 | Failure |
| 13 | 44 | 6.1×10^6 | Survival |
| 14 | 46 | 3.1×10^6 | Failure |
| 15 | 44 | 5.4×10^6 | Survival |
| 16 | 46 | 3.7×10^6 | Failure |
| 17 | 44 | 3.2×10^6 | Failure |
| 18 | 42 | 5×10^6 | Survival |
| 19 | 44 | 5.2×10^6 | Survival |
| 20 | 46 | 2.9×10^5 | Failure |
| 21 | 44 | 5.4×10^6 | Survival |
| 22 | 46 | 1.2×10^6 | Failure |
| 23 | 44 | 5.3×10^6 | Survival |
| 24 | 46 | 1.5×10^6 | Failure |
| 25 | 44 | 5.1×10^6 | Survival |